MKPH-T-04-01

Meson retardation in deuteron electrodisintegration[†]

M. Schwamb and H. Arenhövel
Institut für Kernphysik, Johannes Gutenberg-Universität, D-55099 Mainz, Germany
(Dated: February 8, 2008)

The effect of meson retardation in NN-interaction and exchange currents on deuteron electrodisintegration is studied in a coupled channel approach including NN-, $N\Delta$- and πd-channels. It is shown that the influence of retardation depends on the energy regime: Whereas below π-threshold calculations with static and retarded operators yield almost identical results, they differ significantly in the Δ-region. Especially, the longitudinal and the longitudinal-transverse interference structure functions are strongly affected.
Keywords: Deuteron electrodisintegration; Meson retardation, Meson exchange currents; Δ-Excitation

PACS numbers: 13.40.-f, 21.45.+v, 25.30.Fj

arXiv:nucl-th/0401014v1 9 Jan 2004

I. INTRODUCTION

Recently we have constructed a realistic NN-interaction model and corresponding electromagnetic (e.m.) exchange currents based on a coupled channel approach with meson, nucleon and Δ-degrees of freedom and have applied it to NN-scattering and deuteron photodisintegration [1, 2, 3]. It contains complete meson retardation in both the NN-interaction as well as in the e.m. pionic meson exchange currents (π-MEC). In addition off-shell contributions to the e.m. one-body current were considered in subsequent work [4]. As was shown in [3], the influence of retardation is large above pion threshold and only its incorporation leads to a satisfactory theoretical description of deuteron photodisintegration in the Δ-region. On the other hand, e.m. off-shell effects turned out to be quite small [4].

Due to the possibility of an independent variation of energy and momentum transfer in the space-like region and the existence of a longitudinal polarization of the exchanged virtual photon, it is expected that electrodisintegration of the deuteron will provide additional insights into the hadronic properties of the NN-system. For example, it allows the study of the NN-interaction in the short-range regime independent of the excitation energy in contrast to photodisintegration. Moreover, in quasifree kinematics this reaction is an important tool for the exctraction of nucleon properties like, e.g. the electric form factor of the neutron [5, 6, 7]. For this reason, we have extended our approach to electrodisintegration. In the next section, a brief survey of our model is given. Then, in Sect. III, results are presented and compared to experimental data for some selected kinematics and, finally, some conclusions are drawn.

II. THEORETICAL FRAMEWORK

The model Hilbert space consists of three basic configurations, i.e. two nucleons (NN), one nucleon and one delta ($N\Delta$), and two nucleons and one meson (e.g. $NN\pi$). The basic hadronic interactions are determined by baryon-baryon-meson vertices, where we include as mesons π, ρ, σ, δ, ω, and η. Inserting the vertices into the appropriate Lippmann-Schwinger equation, one obtains after some straightforward algebra [2] the desired retarded one-boson-exchange operators describing the interactions $NN \leftrightarrow NN$, $NN \leftrightarrow N\Delta$, and $N\Delta \leftrightarrow N\Delta$. In our explicit realization, we use for the parametrization of the retarded NN-interaction the Elster potential [8], which includes in addition one-pion loop diagrams as nucleon self energy contributions in order to fulfil unitarity above pion threshold. For this reason, one has to distinguish between bare and physical nucleons. For details we refer to [2]. For the interactions $NN \leftrightarrow N\Delta$ and $N\Delta \leftrightarrow N\Delta$, we take besides retarded pion exchange in addition only static ρ-exchange into account. Moreover, the interaction of two nucleons in the channel with deuteron quantum numbers in the presence of a spectator pion, called πd-channel, is also considered. By a suitable box renormalization [9], an approximate phase equivalence between the Elster potential, which does not include Δ-d.o.f., and our coupled channel approach below pion threshold is obtained. The hadronic Δ-parameters are fitted to the P_{33}-channel of pion-nucleon scattering and the $^1D_2$-channel in NN-scattering. For the sake of comparison with the conventional approach with static interactions,

[†] Supported by the Deutsche Forschungsgemeinschaft (SFB 443).

we have constructed also a static version of our model interaction based on the Bonn OBEPR-potential [10] where in accordance with the usual treatment the pion-nucleon loop diagrams have been neglected. For the results presented below, we have used two of the various model versions discussed in [2], namely "CC(ret,π,ρ,0)" and "CC(stat,π,ρ,0)" for the retarded and static calculations, respectively.

The basic e.m. interaction of the model is described in detail in [3, 4] and consists of baryon and meson one-body currents as well as Kroll-Rudermann (contact) and vertex contributions. These currents are, together with the πNN-vertex, the basic building blocks of the corresponding effective current operators for two baryons consisting of one- and two-body contributions. The matrix element of the effective nucleon one-body operator between plane-wave states of two bare nucleons $\bar{N}$ is given in [4] for real photons. Its extension to virtual photons with four momentum $q^\mu = (\omega, \vec{q})$ reads as follows

$$\begin{aligned}\langle \vec{p}_1',\, \vec{p}_2' \,|J_{eff}^{N[1]\,\mu}(z,\omega,\vec{q})|\vec{p}_1,\, \vec{p}_2\,\rangle \;&=\; \langle \vec{p}_1',\, \vec{p}_2' \,|\frac{\widehat{R}(z)}{\widehat{R}(z^{os})} j_{real}^{N[1]\,\mu}(\omega,\vec{q})\frac{\widehat{R}(z-\omega)}{\widehat{R}(z^{os}-\omega)}|\vec{p}_1,\, \vec{p}_2\,\rangle \\ &\quad + \langle \vec{p}_1',\, \vec{p}_2' \,|\widehat{R}(z)\mathcal{J}_{loop,\,sub}^{\mu}(z,\omega,\vec{q})\widehat{R}(z-\omega)|\vec{p}_1,\, \vec{p}_2\,\rangle\,, \end{aligned} \tag{1}$$

where $j_{real}^{N[1]\,\mu}(\omega,\vec{q})$ denotes the usual nucleon one-body four-current including leading order relativistic contributions like Darwin-Foldy and spin-orbit. They contain e.m. Sachs form factors using the dipole parametrization. Explicit formulas can be found, for example, in [11]. For simplicity, the electric form factor of the neutron is neglected. Furthermore, $z = W + i\epsilon$, and $z^{os} = \sqrt{M_N^2 + (p_1')^2} + \sqrt{M_N^2 + (p_2')^2}$ ($a \equiv |\vec{a}|$ for any vector $\vec{a}$) with $W = \sqrt{M_d^2 + \vec{q}^{\,2}} + \omega$ as invariant mass of the photon deuteron system in the c.m. frame and M_d as deuteron mass. Finally, $\widehat{R}$ denotes the so-called dressing operator describing hadronic off-shell effects [2, 3, 4].

The quantity $\mathcal{J}_{loop,\,sub}^{\mu}$ in (1) denotes the e.m. corrections arising from the pion-nucleon loop which have been discussed in detail in [4] and can be interpreted as e.m. off-shell contributions. For the transition to virtual photons e.m. form factors have to be incorporated. Moreover, the propagators of the loop diagrams with an intermediate $\gamma^*\pi N$-state have to be modified due to the fact that $\omega \neq q$ in electrodisintegration.

For the one-body $(\gamma + \bar{N} \to \Delta)$-transition current, we take the usual nonrelativistic form including only the dominant $M1$-transition

$$\langle \vec{p}_\Delta | \vec{j}_{\Delta\bar{N}}(W_{sub},\omega,\vec{q})|\vec{p}_{\bar{N}}\rangle \;=\; \delta(\vec{p}_\Delta - \vec{p}_{\bar{N}} - \vec{k})\,\frac{e\,\tau_{\Delta\bar{N},\,0}}{2M_N}\widetilde{G}_{M1}^{\Delta\bar{N}}(W_{sub}+i\epsilon,\omega,\vec{q})\,i\vec{\sigma}_{\Delta\bar{N}}\times\vec{q}_{\gamma N}\,, \tag{2}$$

where

$$\vec{q}_{\gamma N} \;=\; \vec{q} - \frac{M_\Delta^{res} - M_N}{M_\Delta^{res}}\,\vec{p}_\Delta \quad \text{with} \quad M_\Delta^{res} = 1232\,\text{MeV}\,. \tag{3}$$

As has been outlined in detail in [3], the e.m. coupling constant $\widetilde{G}_{M1}^{\Delta\bar{N}}$ has been fixed for real photons by a fit of the $M_{1+}^{(3/2)}$-multipole of pion photoproduction on the nucleon. Due to nonresonant rescattering mechanisms, it becomes complex and dependent on the invariant mass W_{sub} of the πN-subsystem for which we adopt the spectator-on-shell approach [3]. Moreover, when embedded into a nuclear medium, $\widetilde{G}_{M1}^{\Delta\bar{N}}$ depends also on the photon momentum $\vec{q}$ and the photon energy ω. As has been shown in [12], at least for photodisintegration a so-called on-shell prescription

$$\widetilde{G}_{M1}^{\Delta\bar{N}}(W_{sub}+i\epsilon,\omega,\vec{q}) \to \widetilde{G}_{M1}^{\Delta\bar{N}}(W_{sub}+i\epsilon) \tag{4}$$

turns out to be very accurate, simplifying considerably the numerical evaluation. The resulting coupling constant used in this paper is parametrized as follows

$$\widetilde{G}_{M1}^{\Delta\bar{N}}(z = W_{sub}+i\epsilon) = \widetilde{\mu}_{\Delta N}(W_{sub})\,e^{i\widetilde{\Phi}(W_{sub})} \tag{5}$$

with

$$\widetilde{\mu}_{\Delta N}(W_{sub}) = \mu_0 + \mu_2\left(\frac{q_\pi}{m_\pi}\right)^2 + \mu_4\left(\frac{q_\pi}{m_\pi}\right)^4 \;\text{ and }\; \widetilde{\Phi}(W_{sub}) = \frac{q_\pi^3}{a_1 + a_2 q_\pi + a_3 q_\pi^2 + a_4 q_\pi^3}\,, \tag{6}$$

where the on-shell pion momentum q_π is a function of W_{sub} according to $W_{sub} = M_N + \frac{q_\pi^2}{2M_N} + \sqrt{m_\pi^2 + q_\pi^2}$, while for $W_{sub} < M_N + m_\pi$ we have set $q_\pi = 0$. The parameters in (6) have been fitted to the resulting coupling constant "$\widetilde{G}_{M1}^{\Delta\bar{N}}$(eff1)" discussed in [3] and are listed in Table I. In addition a contribution from the $\gamma N\Delta$-transtion charge density is included. For virtual photons, again $\widetilde{G}_{M1}^{\Delta\bar{N}}$ must be multiplied with an appropriate e.m. transition form factor

which for simplicity has been chosen in the dipole form. We are aware of the fact that with increasing momentum transfer one finds a slightly stronger fall-off of $\widetilde{G}_{M1}^{\Delta\bar{N}}(Q^2)$ with $Q^2 = q^2 - \omega^2$ compared to the dipole form [13]. However, we restrict ourselves here to kinematics with $Q^2 \leq 4$ fm^{-2} where the difference does not matter.

With respect to the two-body currents, we consider, as in [3], meson retardation in the pure pion exchange contributions whereas retardation in $\gamma\pi\rho/\omega$-MEC turned out to be unimportant in photodisintegration [12], but very CPU-time consuming. Therefore, in order to facilitate our numerical evaluation, we have neglected retardation in the latter contribution. Furthermore, we include in addition static ρ-exchange as well as various Δ-MEC which have been discussed in [3]. Similar to the e.m. loop corrections the transition from photo- to electrodisintegration leads to some modifications in the intermediate $NN\pi\gamma^*$-propagators as well as for the incorporation of an e.m. form factor.

In the static model the e.m. loop contributions $\mathcal{J}^{\mu}_{loop,\,sub}$ to the nucleonic one-body current are neglected naturally and the hadronic dressing factor $\widehat{R}$ is replaced by 1. Obviously, the MEC contain only the usual static terms. Note that in the static limit the recoil contributions do not contribute due to their cancellation against the wave function renormalization [14]. Moreover, in the static limit there are no nonrelativistic MEC-contributions to the charge operator.

For the numerical evaluation of the T-matrix for deuteron electrodisintegration, we use the standard multipole decomposition of the e.m. current. Moreover, we take advantage of Siegert's theorem which allows to express the dominant contributions of the transverse electric multipoles via the charge multipoles.

III. RESULTS AND CONCLUSIONS

Neglecting polarization effects the differential cross section for deuteron electrodisintegration in the one-photon exchange approximation is determined by four structure functions, two diagonal ones f_L and f_T and two interference ones f_{LT} and f_{TT} [15]. They are functions of the squared three momentum transfer q^2 in the c.m. system, the final state c.m.-energy $E_{np} = W - 2M_N$, and the angle θ between $\vec{q}$ and the relative neutron-proton momentum in the final neutron-proton c.m.-system.

We begin the discussion with the experiment of Jordan et al. [16] for the kinematics $E_{np} = 66$ MeV, $q^2 = 3.87$ fm^{-2} which has been performed in order to extract the structure functions f_L, f_T and f_{LT}. Our predictions for these structure functions using both static and retarded operators are shown in Fig. 1 together with the few existing experimental data points. Since this kinematics is well below pion threshold it is not surprising that both approaches yield almost identical results – in fact only for the smallest structure function f_{TT} the corresponding curves can be distinguished – demonstrating that both approaches are indeed equivalent in this kinematic region. A similar result has also been found in photodisintegration [3]. The agreement with experiment is quite satisfactory but more data are certainly needed for a more critical comparison.

The situation changes completely if the excitation energy is above pion threshold. As a first example, we consider in Fig. 2 the kinematics $E_{np} = 179$ MeV, $q^2 = 1.66$ fm^{-2} of an experiment by Turck-Chièze et al. [17]. Whereas f_T is only moderately affected by retardation, the other structure functions, in particular f_L and f_{LT} are much more sensitive to the inclusion of retardation. At forward angles f_L is enhanced by roughly 45 percent while above $\theta \approx 90^\circ$ it is significantly lowered. Especially f_{LT} increases strongly in absolute magnitude. A detailed analysis has shown that this strong retardation effect is mainly due to the charge recoil contribution to the Coulomb monopole (see Fig. 3 for a graphical representation). This is demonstrated in Fig. 2 by the dash-dotted curves for which this contribution is switched off. The remaining retardation effect is significantly smaller. A comparison with the experimental diffferential coincidence cross section is shown in Fig. 4. One readily notes a considerable enhancement of the cross section in the retarded approach improving significantly the agreement with the data. But the agreement is not perfect, the theory being a little too low in the maximum around $\theta_p^{\rm Lab} = 45^\circ$ and somewhat too large at higher angles. Again, the most important contribution of retardation is due to the recoil charge contribution to the monopole.

The importance of retardation becomes even more striking for excitation energies E_{np} in the Δ-region. This is demonstrated in Figs. 5 and 6 for the kinematics of a more recent experiment by Pellegrino et al. [18] with $E_{np} = 280$ MeV and $q^2 = 2.47$ fm^{-2}. The effects of retardation on f_L anf f_{LT} in Fig. 5 are even stronger than in the previous example. However, in the differential cross section the retardation effects in the different structure functions appear to cancel each other to a large extent so that static and retarded approaches yield very close results in the measured angular range $95^\circ < \theta < 135^\circ$ (see Fig. 6) but lead to a slight underestimation of the experiment. The better agreement between theory and experiment reported in [18] is obtained by the use of a modified $\gamma N\Delta$-coupling which is considerably stronger than ours given in Table I due to the assumption of a vanishing nonresonant contribution to the $M_{1+}^{(3/2)}$-multipole. However, as has been discussed in [3], this approach causes formal inconsistencies and is, therefore, questionable.

Comparing the static as well the retarded results for f_{TT} in Fig. 6 to experimental data, one notes a sizable

underestimation of both approaches. This discrepancy may have different origins. First of all, one has to be aware of the fact that the majority of the data (full circles in the right panel of Fig. 6) has been extracted under the assumption $f_{LT} = 0$ which is well justified only in the static, but not all in the retarded approach. Only the open square data points have been obtained without this assumption. Concerning the theoretical uncertainties, the present approach does not contain all relativistic contributions of leading order in p/M_N as is the case in the approach, for example, of Ritz et al. [19]. On the other hand, among the relativistic contributions retardation effects are unique with respect to the singularity structure of the corresponding meson-nucleon propagators above pion threshold which cannot be treated within a Taylor expansion in p/M_N. Therefore, concerning the role of retardation, the approach of [19] cannot be considered realistic above pion threshold. However, the model of Ritz et al. is useful to estimate the role of boost effects (which do not contain any singularities) which are still missing in the present approach. It turns out that for the kinematics of Fig. 6 they are small. Moreover, we have checked that additional, not yet included mechanisms like static σ- or δ-MEC, a nonvanishing G_{En} or a possible $E2$-excitation of the Δ are small and cannot explain the noted discrepancy between theory and experiment in Fig. 6.

In summary, we have studied the role of retardation effects in electrodisintegration of the deuteron for various kinematics. It turns out that especially the recoil charge contribution to the monopole, which is not present in static approaches, is very important for excitation energies above pion threshold, leading to dramatic changes in the structure functions f_L and f_{LT} whereas the other structure functions f_T and f_{TT} are much less affected.

With respect to future developments, one important step concerns an improved treatment of the final-state-interaction. As has already been noted in [2], the description of the phase shifts in several NN-partial waves is only fairly well above pion threshold for our NN-interaction model. This touches a general problem of realistic NN-interactions: In contrast to the energy regime below pion threshold, at present no "high precision" NN-interaction is available for energies above pion threshold. However, this is an indispensable ingredient for any theoretical description of e.m. reactions on the deuteron above pion threshold like photo- or electrodisintegration, but also meson production on the deuteron. A further interesting topic will be the study of polarization observables which supposedly are more sensitive to interaction effects.

[1] M. Schwamb, H. Arenhövel, P. Wilhelm, Th. Wilbois, Phys. Lett. B 420 (1998) 255.
[2] M. Schwamb, H. Arenhövel, Nucl. Phys. A 690 (2001) 647.
[3] M. Schwamb, H. Arenhövel, Nucl. Phys. A 690 (2001) 682.
[4] M. Schwamb, H. Arenhövel, Nucl. Phys. A 696 (2001) 556.
[5] C. Herberg et al., Eur. Phys. J. A 5 (1999) 131.
[6] M. Ostrick et al., Phys. Rev. Lett. 83 (1999) 276.
[7] I. Passchier et al., Phys. Rev. Lett. 82 (1999) 4988.
[8] Ch. Elster, W. Ferchländer, K. Holinde, D. Schütte, R. Machleidt, Phys. Rev. C 37 (1988) 1647.
[9] A. M. Green, M. E. Saino, J. Phys. G 8 (1982) 1337.
[10] R. Machleidt, K. Holinde, Ch. Elster, Phys. Rep. 149 (1987) 1.
[11] T. Wilbois, G. Beck, H. Arenhövel, Few Body Sys. 15 (1993) 39.
[12] M. Schwamb, PhD-Thesis, Mainz 1999.
[13] L. Tiator, D. Drechsel, S.S. Kamalov, S.N. Yang, Eur. Phys. J. A 17 (2003) 357.
[14] M. Gari, H. Hyuga, Z. Phys. A 277 (1976) 291.
[15] W. Fabian, H. Arenhövel, Nucl. Phys. A 314 (1979) 253.
[16] D. Jordan et al., Phys. Rev. Lett. 76 (1996) 1579.
[17] S. Turck-Chièze et al., Phys. Lett. B 142 (1984) 145.
[18] A. Pellegrino et al., Phys. Rev. Lett. 78 (1997) 4011.
[19] F. Ritz, H. Göller, T. Wilbois, H. Arenhövel, Phys. Rev. C 55 (1997) 2214.

TABLE I: Parameters of the $\gamma N\Delta$-coupling in (6).

μ_0	μ_2	μ_4	a_1 [fm^{-3}]	a_2 [fm^{-2}]	a_3 [fm^{-1}]	a_4
5.0912	0.017511	−0.017652	0.5564	5.4317	−3.5987	3.8491

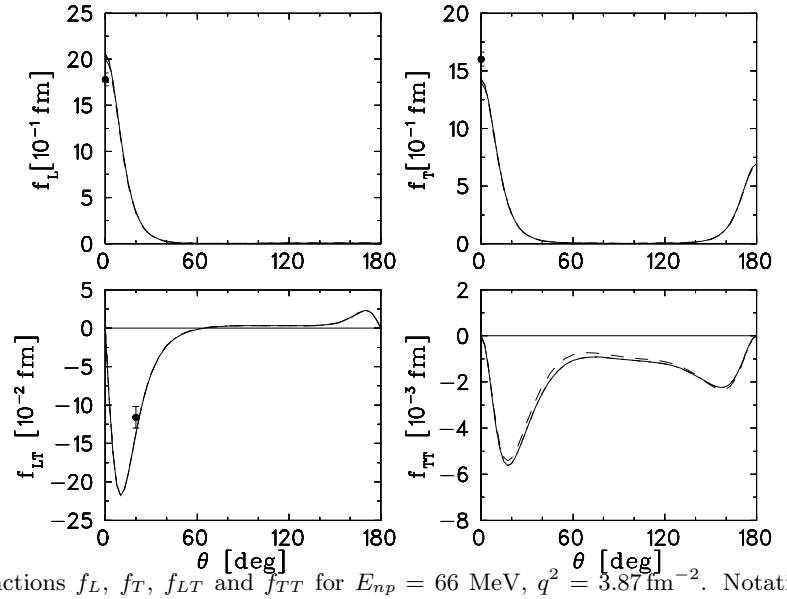

FIG. 1: The structure functions f_L, f_T, f_{LT} and f_{TT} for $E_{np} = 66$ MeV, $q^2 = 3.87\,\mathrm{fm}^{-2}$. Notation of the curves: dashed: static approach; full: retarded approach. Experimental data from [16].

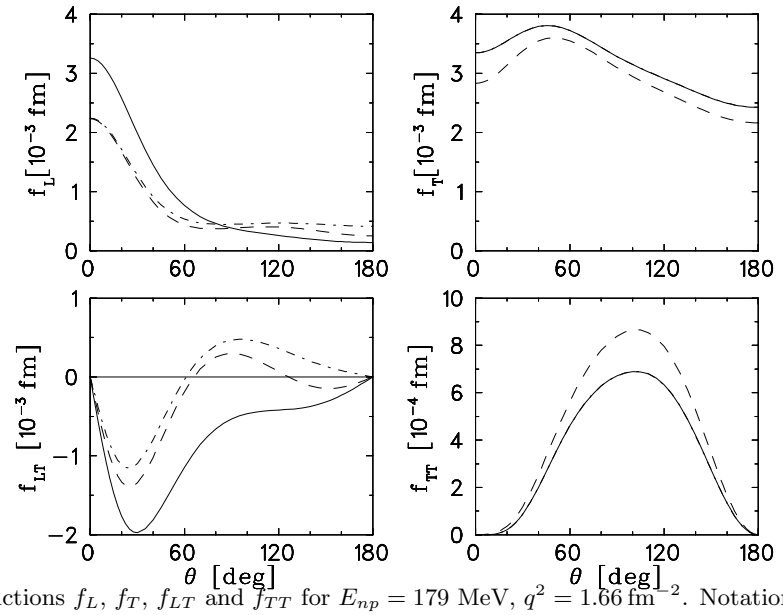

FIG. 2: The structure functions f_L, f_T, f_{LT} and f_{TT} for $E_{np} = 179$ MeV, $q^2 = 1.66\,\mathrm{fm}^{-2}$. Notation of the curves as in Fig. 1. The additional dash-dotted curves represent the results of the retarded approach where the Coulomb monopole contribution of the recoil charge operator is switched off.

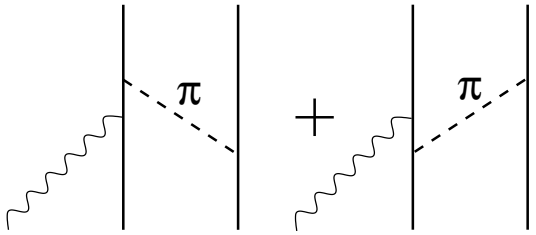

FIG. 3: Diagrammatic representation of the recoil contributions to the effective charge and current operators. The coupling of the photon to the nucleon is given solely by the nonrelativistic charge and spin/convection current, respectively.

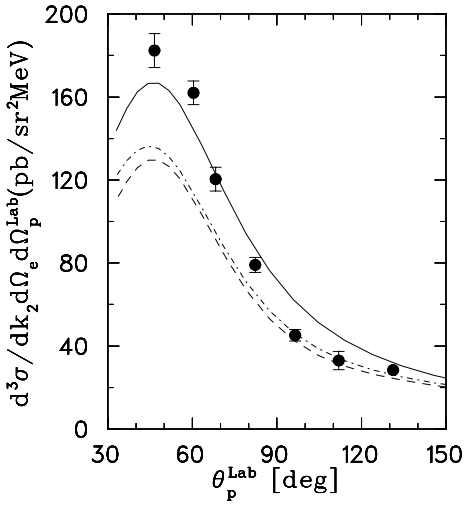

FIG. 4: The lab frame differential cross section for $E_{np} = 179$ MeV, $q^2 = 1.66\,\mathrm{fm}^{-2}$ and an electron scattering angle of $\theta_e^{Lab} = 25^\circ$. The lab angle of the outgoing proton is denoted by θ_p^{Lab}. Experimental data from [17].

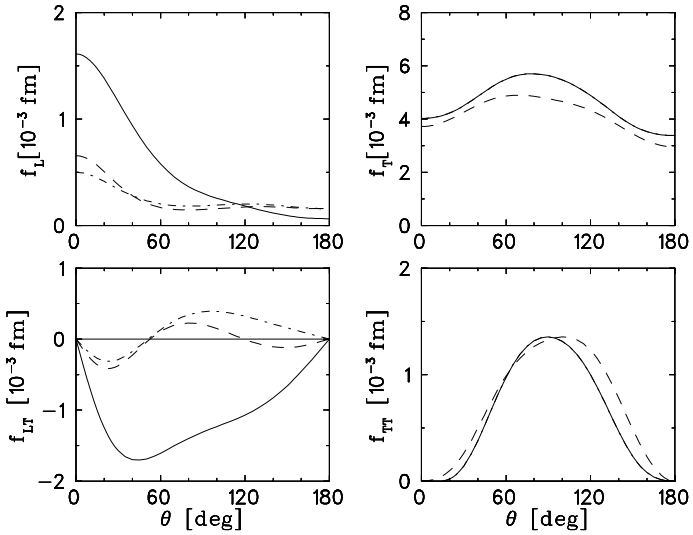

FIG. 5: The structure functions f_L, f_T, f_{LT} and f_{TT} for $E_{np} = 280$ MeV, $q^2 = 2.47$ fm^{-2}. Notation of the curves as in Fig. 2.

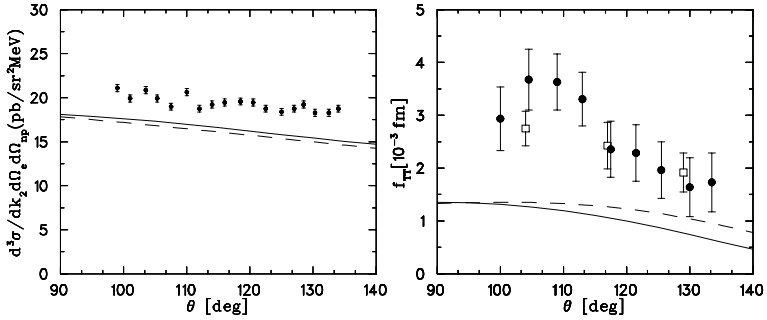

FIG. 6: The differential cross section (left panel) and the f_{TT}-structure function (right panel) for $E_{np} = 280$ MeV, $q^2 = 2.47$ fm$^{-2}, \theta_e = 30^\circ$. Notation as in Fig. 1. Experimental data from [18].